Journal of Solid State Chemistry **145,** 182–185 (1999)
Article ID jssc.1999.8239, available online at http://www.idealibrary.com on IDEAL®

Low-Temperature Phase of Sodium Priderite, $Na_xCr_xTi_{8-x}O_{16}$, with a Monoclinic Hollandite Structure

Yuichi Michiue, Akira Sato, and Mamoru Watanabe

National Institute for Research in Inorganic Materials, Namiki 1-1, Tsukuba, Ibaraki 305-0044, Japan

Received November 20, 1998; in revised form February 19, 1999; accepted February 23, 1999

Sodium priderite, $Na_xCr_xTi_{8-x}O_{16}$ ($x \approx 1.7$) having a tetragonal hollandite structure, undergoes monoclinic distortion below ca. 273 K. The monoclinic phase structure, the space group *12/m*, and cell parameters $a=10.108(7)$, $b=2.9526(4)$, and $c=9.975(7)$ Å, and $\beta=90.06(4)^\circ$ with $Z=1$, were refined using data measured at 223 K through single-crystal X-ray diffraction ($R=5.1$, $wR=5.7\%$). Electron density maps drawn using the maximum entropy method clearly show variations in asymmetry in the Na ion distribution in the tunnel associated with monoclinic deformation of the framework. A marked difference between the monoclinic and tetragonal structures is the inequality of Na occupation ratios among the four positions in a cavity.

Key Words: **Sodium priderite; hollandite structure; one-dimensional tunnel; low-temperature X-ray diffraction; maximum entropy method (MEM); electron density distribution.**

INTRODUCTION

Priderite is a member of a large family having a hollandite structure that is characterized by a host framework containing one-dimensional tunnels constructed from infinite chains of pseudocuboctahedral cavities formed by oxygen atoms. Of the numerous compounds having a hollandite structure, sodium priderite has unique structural features (1,2) caused by the small size of its tunnel ion (i.e., Na) compared to ordinary hollandite compounds having K, Rb, and Cs as tunnel ions. Na ions are found, for example, both in the cuboctahedral cavity and at the bottleneck coordinated by four oxygen atoms square planarly, which forms the connection plane between adjacent cavities. Tunnel ions in cavities distinctly deviate from the center in directions normal to the tunnel axis, which has never been observed in other compounds having a hollandite structure. This unique ion distribution was well reproduced by molecular dynamics simulation using classical pair potentials (3).

Such delocalization is presumably sensitive to temperature change, which may be expected to reflect the stability of the crystal structure. A study of the temperature dependence of Na ion distribution showed a phase transition from tetragonal to monoclinic at low temperature. The compositionally varied tetragonal–monoclinic transformation of a hollandite structure was found in some solid-solution systems such as $Ba_{1.23}(AlTi)_8O_{16}$–$Ba_{1.28}(FeTi)_8O_{16}$ (4). To our knowledge, however, sodium priderite is the first example of a compound having a hollandite structure showing isomorphous transformation from tetragonal to monoclinic as a low-temperature phase.

EXPERIMENTAL

A single crystal of tetragonal sodium priderite from the same run as our previous study (1) was mounted on an automated four-circle diffractometer (Enraf-Nonius CAD-4) to collect intensity data at 223 K. Table 1[1] lists crystallographic data and conditions for data collection and refinement based on F. Atomic scattering factors are from International Tables for X-Ray Crystallography, Vol. IV (5) using programs ACACA (6), RADY (7), RSSFR-5 (8), and BADTEA (9).

Electron density maps were drawn using the maximum entropy method (MEM) (10–12) as in the tetragonal phase (2); 1487 independent reflections having phases given by least-squares refinement were used for constraints. The unit cell was divided into $64 \times 32 \times 64$ pixels and total electrons fixed at $F(000)$ ($= 326$). A set of electron densities at pixels satisfying $C/N < 1$ was obtained after 3023 iterations from a flat distribution, where $C = \sum_k |F_c(k) - F_0(k)|^2/\sigma(k)^2$ and N is the number of reflections, i.e., 1487. Final reliability factor R was 1.75% and wR, 1.79%. Calculations were performed using the program MEED (13).

RESULTS AND DISCUSSION

The monoclinic framework is distorted slightly from the fourfold symmetry of the tetragonal structure ($a = b =$ 10.058(1), $c = 2.957(1)$ Å). The a-axis is elongated and the

[1]Structure factor tables are available on request from the authors.

0022-4596/99 $30.00

TABLE 1
Crystallographic Data and Conditions for Data Collection and Refinement for Monoclinic Sodium Priderite, $Na_xCr_xTi_{8-x}O_{16}$ ($x \approx 1.7$)

Temperature (K)	223
M_r	685.4
Crystal system	Monoclinic
Space group	$I2/m$
a (Å)	10.108(7)
b	2.9530(4)
c	9.975(7)
β (°)	90.06(4)
V [Å^3]	297.7(3)
Z	1
Dx (g/cm^3)	3.8
μ(Mo$K\alpha$) (cm^{-1})	55.9
Crystal size (mm)	$0.07 \times 0.07 \times 0.2$
Color	Dark green
Radiation	Mo$K\alpha$ (0.71069 Å) (graphite-monochromatized)
Refinement of cell parameters	22 reflections ($48° \le 2\theta \le 58°$)
Scan mode	$\omega - 2\theta$
$2\theta_{max}$	100° ($-21 \le h \le 21$, $0 \le k \le 6$, $0 \le l \le 21$)
Standard reflections	2 every 200 (variation within 1.4%)
Reflections measured	1792
Reflections used for calculation	1487 ($F_0 > 3\sigma(F_0)$)
Absorption correction	Numerical
Transmission factor	0.605–0.705
Final R, wR	0.0509, 0.0569 (weight factor: $1/\sigma(F_0)^2$)
$\Delta\rho_{min}$, $\Delta\rho_{max}$	-1.6, 5.7 (e/Å^3)

TABLE 2
Occupancies, Atomic Coordinates, and Thermal Parameters for Monoclinic Sodium Priderite

Atom	Multiplicity	Occupancy	x	y	z	B_{eq}(Å^2)[a]
Na1^i	4	0.136(5)	0.079(2)	0.5	0.012(2)	2.9(8)
Na1^{ii}	4	0.078(7)	0.987(3)	0.5	0.070(4)	5.5(28)
Na2	8	0.076(6)	0.020(2)	0.200(10)	0.000(4)	4.8(19)
Na3	2	0.12(3)	0	0	0	4.3(39)
M^i (Ti/Cr)	4	0.786/0.214	0.35255(5)	0	0.16978(5)	0.50(1)
M^{ii} (Ti/Cr)	4	0.786/0.214	0.83172(5)	0	0.35105(5)	0.51(1)
O1^i	4	1	0.1549(2)	0	0.2005(2)	0.38(5)
O1^{ii}	4	1	0.7968(2)	0	0.1531(2)	0.38(5)
O2^i	4	1	0.5421(2)	0	0.1672(2)	0.48(5)
O2^{ii}	4	1	0.8379(2)	0	0.5420(2)	0.46(5)

Atom	β_{11}[b]	β_{22}	β_{33}	β_{13}
Na1^i	57(15)	129(32)	47(14)	16(12)
Na1^{ii}	55(33)	305(144)	89(48)	−2(32)
Na2	25(28)	232(88)	135(40)	35(33)
Na3	10(30)	317(270)	34(25)	2(19)
M^i (Ti/Cr)	140(3)	44(3)	197(4)	54(3)
M^{ii} (Ti/Cr)	165(3)	40(3)	182(4)	−16(3)
O1^i	120(12)	13(12)	155(14)	31(10)
O1^{ii}	107(11)	16(12)	163(13)	25(10)
O2^i	92(12)	50(13)	226(15)	29(11)
O2^{ii}	182(13)	40(13)	125(13)	−9(10)

[a] Temperature factors take the form $\exp[-(h^2\beta_{11} + k^2\beta_{22} + l^2\beta_{33} + 2hk\beta_{12} + 2hl\beta_{13} + 2kl\beta_{23})]$, $B_{eq} = (4/3)\sum_i\sum_j \beta_{ij}a_ia_j$.
[b] β_{11}, β_{33}, and β_{13} are multiplied by 10^4 for Na atoms and by 10^5 for others, β_{22} are multiplied by 10^3 for Na atoms and by 10^4 for others. $\beta_{12} = \beta_{23} = 0$.

c-axis shortened compared to that of the tetragonal phase while maintaining angle β at nearly 90°. Table 2 lists atomic coordinates, occupancies, and equivalent isotropic temperature factors of monoclinic $Na_xCr_xTi_{8-x}O_{16}$ ($x \approx 1.7$) at 223 K. Nonequivalent atoms equivalent in the tetragonal phase are distinguished from each other by superscript i or ii. The tunnel is constructed by alternate stacking of two types of oxygen pseudosquares along the b axis. The smaller square consists of two O1^i and two O1^{ii} oxygen atoms each and the larger square consists of two O2^i and two O2^{ii} atoms; analogous to the tetragonal phase, the former is called O1-pseudosquare and the latter O2-pseudosquare. The cuboctahedral cavity in the tunnel is formed by 8O1 and 4O2. Table 3 compares interatomic distances between the two forms. Differences are significant for M–O2 distances.

Na ions occur at four positions Na1^i, Na1^{ii}, Na2, and Na3 in the tunnel, similar to those in the tetragonal structure. Na1^i and Na1^{ii} are on the O2-pseudosquare plane, showing significantly varied site occupancy. The occupation ratio increases at Na1^i and decreases at Na1^{ii}, although these sites have the same 0.11 in the tetragonal phase. The Na1^i site also deviates 0.81(2) Å from the tunnel center, compared to 0.74(2)Å in the tetragonal form, and Na1^{ii} changes little (0.73(4) Å). Oxygen coordination distances of the Na1^i site are therefore shorter in the monoclinic than in the tetragonal structure, whereas distances of the Na1^{ii} site are similar within the error between the two phases (Table 3). Na densities at Na1^i and Na1^{ii} sites clearly differ as the electron density map shows at $y = 1/2$ (Fig. 1c). Na2 resides

TABLE 3
Interatomic Distances (Å) for Sodium Priderite

Monoclinic				Tetragonal	
M^i–O1^i	2.021 (2)	M^{ii} –O1^{ii}	2.006(3)	M –O1	2.012(2)
–O1^i × 2	1.964 (2)	–O1^{ii} × 2	1.967(1)	–O1 × 2	1.964(1)
–O2^i	1.916(2)	–O2^{ii}	1.906(3)	–O2	1.925(2)
–O2^{ii} × 2	1.956(2)	–O2^i × 2	1.959(1)	–O2 × 2	1.953(1)
Average	1.963(2)	Average	1.961(2)	Average	1.962(1)
Na1^i–O1 × 2	2.51 (1)	Na1^{ii} –O1^{ii} × 2	2.56(3)	Na1 –O1 × 2	2.54(2)
–O1^{ii} × 2	2.55 (1)	–O1^i × 2	2.60(3)	–O1 × 2	2.60(2)
–O2^{ii}	2.63(2)	–O2^i	2.63(4)	–O2	2.66(2)
Na2 –O1^i	2.49(3)	Na3 –O1^i × 2	2.542(3)	Na2 –O1 × 4	2.634(7)
–O1^i	2.74(3)	–O1^{ii} × 2	2.558(3)		
–O1^{ii}	2.47(3)			Na3 –O1 × 4	2.565(2)
–O1^{ii}	2.78(2)				

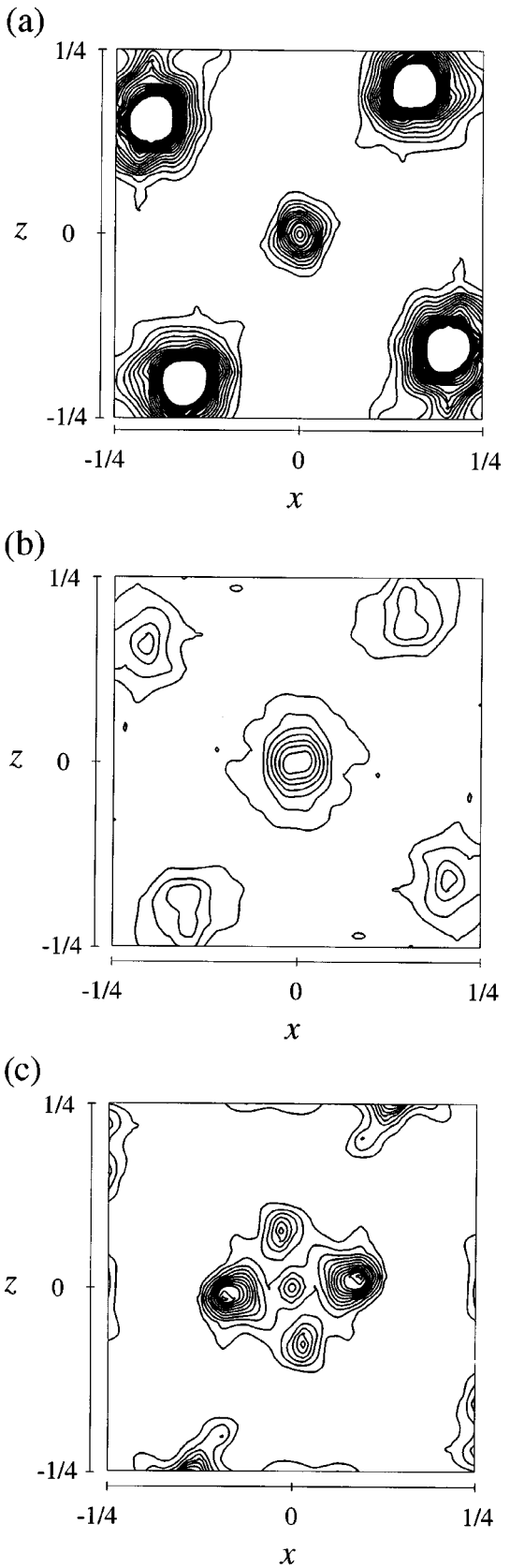

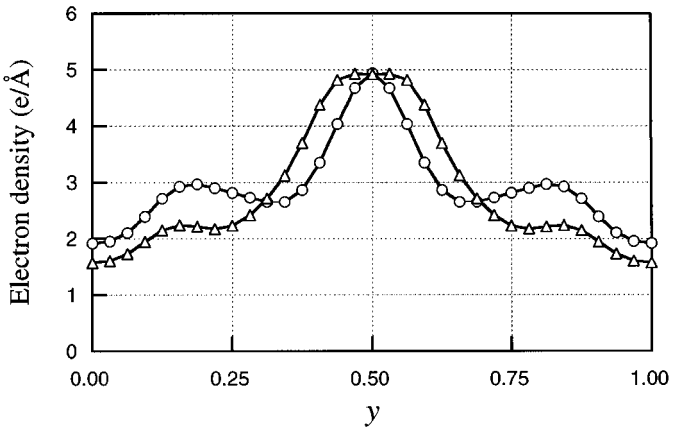

FIG. 2. Electron density along the tunnel based on the analysis using the maximum entropy method for monoclinic (○) and tetragonal (△) sodium priderite. Electrons within $(x^2 + z^2)^{1/2} < 0.12$ are summed up at each y level.

on the tunnel axis in the tetragonal structure but slightly off the axis in the monoclinic structure, consistent with the peak shape in the electron density map near $y = 0.20$ (Fig. 1b). Unique to sodium priderite, large amounts of Na ions are found at the center of the O1-pseudosquare, i.e., the Na3 site. The electron distribution at this site does not indicate the peak splitting shown in Fig. 1(a). Priderites with a large alkali ion such as K, Rb, or Cs force tunnel ions away because the site is subject to O1-square bottlenecking.

The electron density distribution along the tunnel was calculated from MEM analysis, i.e., electrons in the range of

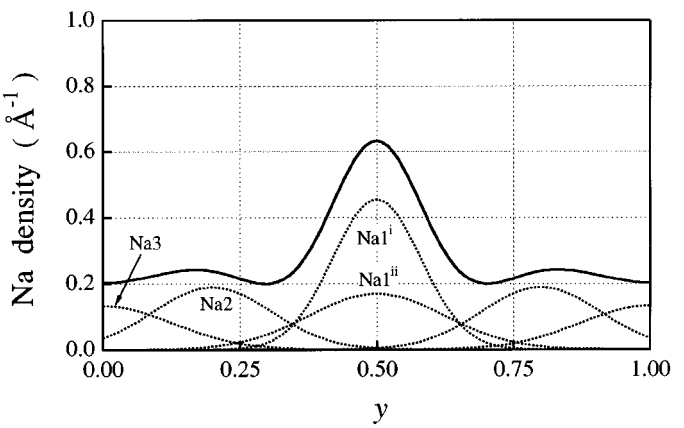

FIG. 3. Na density along the tunnel drawn using parameters from least-squares refinement for monoclinic sodium priderite. Dotted lines are densities for individual Na ions.

FIG. 1. Contour maps of electron densities in monoclinic sodium priderite obtained using the maximum entropy method. (a) $y = 0$, (b) $y = 7/32$, and (c) $y = 1/2$. Contour intervals are 0.4 e/Å^3. Four strong peaks near corners in (a) are due to O1^{i} and O1^{ii} oxygen atoms. Contours are omitted in ranges exceeding 10 e/Å^3.

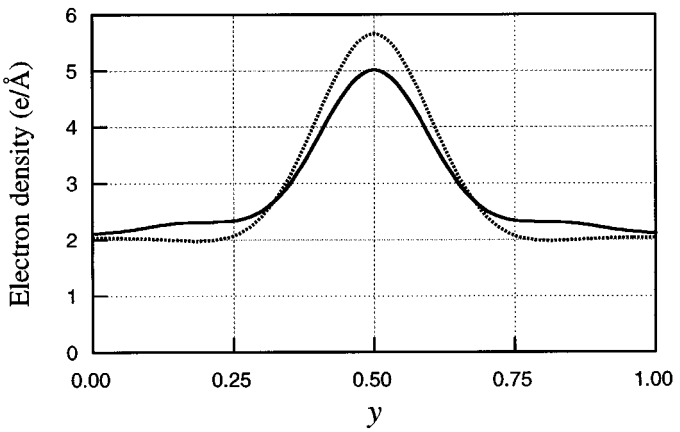

FIG. 4. Electron density along the tunnel based on least-squares refinement for monoclinic (solid line) and tetragonal (dotted line) sodium priderite.

$(x^2 + z^2)^{1/2} < 0.12$ are summed up on a y level at 1/32 intervals and the result compared to that of the tetragonal phase in Fig. 2. Density increases in the range of $-0.31 < y < 0.31$ and decreases in the range of $0.31 < y < 0.69$ after phase transition from tetragonal to monoclinic, indicating that Na ions remain preferably at open cavities at higher temperatures. We drew the Na ion density along the tunnel using parameters from least-squares refinement

$$\rho_{Na}(y) = \sum_n c_n (2\pi U_{22n})^{-1/2} \exp\{-y_n - y)^2/2U_{22n}\},$$

where c_n is the occupation ratio, y_n the fractional coordinate, and U_{22n} ($= \beta_{22n}/2\pi^2 b^{*2}$) the thermal parameter of the nth Na ion. Large U_{22} resulted in a continuous distribution (Fig. 3). Positional disordering, rather than thermal vibration, may actually be the main factor for large thermal parameters even at this temperature. The Na ion density (Fig. 3) was converted to the electron density by convoluting the electron distribution function for one Na ion. The resultant distribution (Fig. 4) significantly differs from that based on the MEM (Fig. 2). The temperature dependence of the electron distribution is, however, qualitatively common. The discrepancy between results from the two methods is mainly due to the fact that conventional least-squares refinement is based on a structure model in which the probability density function of each atom is, according to harmonic vibration approximation, confined to the Gaussian (Fig. 3), whereas the MEM is free of the atomicity concept, giving the set of electron densities as a least-biased deduction compatible with given information, i.e., structure factors.

REFERENCES

1. Y. Michiue and M. Watanabe, *J. Solid State Chem.* **116,** 296 (1995).
2. Y. Michiue and M. Watanabe, *Solid State Ionics* **79,** 116 (1995).
3. Y. Michiue and M. Watanabe, *J. Phys. Chem. Solids* **57,** 547 (1996).
4. R. W. Cheary, *Acta Crystallogr. B* **42,** 229 (1986).
5. "International Tables for X-Ray Crystallography," Vol. IV. Kynoch Press, Birmingham, 1974.
6. B. J. Wuensch and C. T. Prewitt, *Z. Kristallogr.* **122,** 24 (1965).
7. S. Sasaki, "RADY, Program Derived from ORFLS and RADIEL," State Univ. of New York, Stony Brook, New York, 1982.
8. T. Sakurai, "The Universal Crystallographic Computation Program System," The Crystallographic Society of Japan, Tokyo, 1967.
9. L. W. Finger and E. Prince, Tech. Note No. 854. U.S. National Bureau of Standards (1975).
10. S. F. Gull and G. J. Daniell, *Nature* **272,** 686 (1978).
11. D. M. Collins, *Nature* **298,** 49 (1982).
12. M. Sakata and M. Sato, *Acta Crystallogr. A* **46,** 263 (1990).
13. S. Kumazawa, Y. Kubota, M. Takata, and M. Sakata, *J. Appl. Crystallogr.* **26,** 453 (1993).